

An Experimental Investigation on Condensation in Horizontal Microchannels

Minhhung Doan, Thanhtrung Dang

Department of Thermal Engineering, Hochiminh City University of Technology and Education, Vietnam

Abstract — This paper presented an experimental study on condensation in two horizontal microchannel condensers (M1 and M2) with different substrate and channel lengths. The mass flow rate of steam and pressure drop affected to oscillation of condensation profile, beginning condensation point, and performance index. Moreover, heat transfer rate of model M1 was higher than that of model M2 at the same flow rate or pressure drop of steam. The heat transfer rate of 164 W was achieved for the model M1 at inlet vapor temperature of 101.9 °C. Besides, the pressure drop obtained from the microchannel condenser M1 was lower than that obtained from the microchannel condenser M2: at mass flow rate of 0.0264 g/s, the pressure drop of M1 was 1,257 Pa while the pressure drop of M2 was 6,105 Pa. In addition, the performance index decreased as rising mass flow rate of steam for both condensers. With the microchannel condenser M1, the performance index was decreasing from 0.053 W/Pa to 0.038 W/Pa as varying mass flow rate of steam from 0.0264 g/s to 0.0314 g/s. The performance indexes decreased linearly for both condensers.

Keywords— Condensation, heat transfer, microchannel, pressure drop, temperature.

I. INTRODUCTION

Heat transfer and fluid flow phenomena of two phase flow in microchannels are interesting topics in recent years. Regarding to the fields, Sur and Liu [1] studied adiabatic air - water two-phase flow in circular microchannels. Four basic flow patterns (bubbly flow, slug flow, ring flow and annular flow) were observed with inner diameters of 100, 180 and 324 μm . The effects of channel size and superficial phasic velocity on the two-phase flow pattern and pressure drop of air-water mixture were done experimentally. Results shown the flow

pattern-based models provide the best prediction of the two-phase pressure drop in the microchannels.

Choi et al. [2] investigated adiabatic two-phase flow in rectangular microchannels with different aspect ratios: the aspect ratios of the rectangular microchannels were 0.92, 0.67, 0.47 and 0.16; and the hydraulic diameters of the rectangular microchannels were 490, 490, 322 and 143 μm , respectively. In this study, as the aspect ratio decreased, the bubble flow regime became dominant due to the confinement effect and the thickness of liquid film in corner was decreased. The two-phase flow becomes homogeneous with decreasing aspect ratio owing to the reduction of the liquid film thickness. Choi et al. [3] also studied adiabatic two-phase flow in rectangular microchannels with different aspect ratios for bubble behaviors and pressure drop in single bubble. Results shown that the pressure drop in the single elongated bubble in the rectangular microchannel increased as the aspect ratio decreased.

Comparison of condensation heat transfer and pressure drop of CO_2 in microchannels was presented by Heo et al. [4]. The channels were rectangular; the hydraulic diameters were 1.5, 0.78, and 0.68 mm for the 7, 23, and 19 ports, respectively. Increasing and decreasing the heat transfer coefficient at critical vapor quality was observed for the microchannel of 23 ports and the highest pressure drop was found in the microchannel of 23 ports.

Mghari et al. [5] studied condensation heat transfer in horizontal non-circular microchannels. For this study, the conservation equations of mass, momentum and energy numerically solved in both phases (liquid and vapor), and all the more so the film thickness analytical expression established. Mathematical model was used with one channel only. Using annular flow model, the effect of the microchannel shapes on the average Nusselt number was highlighted by studying condensation of steam in square, rectangular and equilateral triangular microchannels with

Nomenclature

A	heat transfer area [m^2]
A_c	cross-sectional area [m^2]
c	specific heat at constant pressure [$\text{J}/(\text{kgK})$]
D_c	depth of channel [m]
D_h	hydraulic diameter [m]

R_{conv}	convective thermal resistance [$\text{m}^2\text{K}/\text{W}$]
Re	Reynolds number
T	temperature [$^\circ\text{C}$]
w	velocity in the z-direction [m/s]
W	width of substrate [m]
W_c	width of microchannel [m]

f	Fanning friction factor	r	latent heat of condensation [kJ/kg]
h_c	convective heat transfer coefficient of the cold side [W/(m ² K)]	<i>Greek symbols</i>	
h_h	convective heat transfer coefficient of the hot side [W/(m ² K)]	ρ	density [kg/m ³]
k	overall heat transfer coefficient [W/(m ² K)]	μ	dynamic viscosity [kg/(ms)]
L	length of substrate [m]	ε	effectiveness (NTU method)
L_c	channel length [m]	δ	thickness of heat transfer [m]
m	mass flow rate [kg/s]	λ	thermal conductivity [W/(mK)]
P	wetted perimeter [m]	Δp	pressure drop of hot side [Pa]
q	heat flux [W/m ²]	Δp_h	pressure drop of hot side [Pa]
Q	heat transfer rate [W]	Δp_t	total pressure drop [Pa]
Q_c	heat transfer rate of the cold side [W]	ΔT_{lm}	log mean temperature difference [°C]
Q_h	heat transfer rate of the hot side [W]	ΣR	overall thermal resistance [m ² K/W]
Q_i	internal heat generation [W/m ³]	ξ	performance index [W/kPa]
Q_{loss}	heat loss rate [W]		
R_{cond}	conductive thermal resistance [m ² K/W]		

the same hydraulic diameter of 250 μm . Mghari et al. [6] enhanced the models in [5] by decreasing hydraulic diameter for a non-circular microchannel. Reducing the microchannel hydraulic diameter from 250 to 80 μm reduced the condensate film thickness and increased the average heat transfer coefficient up to 39% for the same mass flux. The enhancement factor of the heat transfer coefficient reached 100% by increasing the contact angle from 6 to 15°. The influence of the microchannel shape on the condensation heat transfer was highlighted also. The results shown the lowest average Nusselt numbers are obtained for the square microchannel.

Quan et al. [7] experimentally studied steam condensation in silicon microchannels having hydraulic diameters of 109 μm , 142 μm , 151 μm , and 259 μm . It was observed that decreasing friction pressure drop of two phase flow was effected strongly by hydraulic diameter, mass flow rate, and vapor quality. The experimental results were compared with correlation equations, with error of $\pm 15\%$. Inheriting the model in [7], annular condensation heat transfer coefficient of steam in microchannels with trapezoidal cross sections was also determined by Quan et al. [8], having hydraulic diameters of 173 μm and 127 μm with the same aspect ratio of 3.15. In this study, a semi-analytical method, based on turbulent flow boundary layer theory of liquid film with correlations of pressure drop and void fraction valid for microchannels, was used to derive the annular local condensation heat transfer coefficients. The predicted values based on the semi-analytical model were found within $\pm 20\%$ of 423 data points. The annular condensation heat transfer coefficient in microchannels was found to be increasing with mass

flux and quality, but decreasing with the hydraulic diameter.

Dang and Doan [9] experimentally studied condensation heat transfer of microchannel heat exchangers. The condensation heat transfer coefficient in the microchannel heat exchangers decreased as increasing the inlet cooling water temperature. The results for two phases were in good agreement with the results for single phase.

From the relevant literatures above, authors did not mention oscillation of condensation profile, beginning condensation point, and performance index. So, it is important to experimentally investigate on condensation in horizontal microchannels with effects of the pressure drop and mass flow rate of steam. In the following sections, the heat transfer and pressure drop phenomena of the two Aluminum microchannel condensers will be investigated. All experimental conditions of two heat exchangers are the same.

II. METHODOLOGY

Design and fabrication

To design and fabricate the two microchannel condensers, the assumptions were made:

- Heat transfer is steady state
- Radiation heat transfer is negligible
- Two condensers were designed and fabricated by a precision micromachining process; as a result of this manufacturing process, roughness of microchannels was of the same order.

For the experiments carried out in this study, the effects of various parameters on the heat transfer and fluid flow – such as temperature, heat transfer rate, pressure drop, and performance index – of the heat exchangers are discussed

as follows.

The energy balance equation for microchannel condensers is expressed by:

$$m_v c_v (T_{v,i} - T_{v,o}) + r = m_w c_w (T_{w,o} - T_{w,i}) \quad (1)$$

The maximum heat transfer rate, Q_{max} , is evaluated by

$$Q_{max} = (mc)_{min}(T_{v,i} - T_{w,i}) \quad (2)$$

The heat transfer rate of the heat exchanger, Q , is calculated by

$$Q_w = m_w c_w (T_{w,o} - T_{w,i}) \quad (3)$$

The effectiveness (NTU method) is determined by

$$\varepsilon = \frac{Q_w}{Q_{max}} \quad (4)$$

Heat flux is calculated by

$$q = \frac{Q_w}{A} = \frac{m_w c_w (T_{w,o} - T_{w,i})}{nL_w W_w} \quad (5)$$

$$\text{Or } q = k \Delta T_{lm} = \frac{\Delta T_{lm}}{\Sigma R} \quad (6)$$

The overall thermal resistance ΣR is determined by

$$\Sigma R = R_{cond} + R_{conv} \quad (7)$$

The log mean temperature difference is calculated by

$$\Delta T_{lm} = \frac{\Delta T_{max} - \Delta T_{min}}{\ln \frac{\Delta T_{max}}{\Delta T_{min}}} \quad (8)$$

where m is mass flow rate (subscripts v and w stand for the vapor and water sides, respectively), n is number of microchannels, c is specific heat, $T_{v,i}$, $T_{v,o}$, $T_{w,i}$ and $T_{w,o}$ are inlet and outlet temperatures of the vapor and water sides, respectively, r is latent heat, q is heat flux, A is heat transfer area, k is overall heat transfer coefficient,

$R_{cond} = \frac{\delta}{\lambda}$ is conductive thermal

resistance, $R_{conv} = \frac{1}{h_h} + \frac{1}{h_c}$ is convective thermal

resistance, h_v and h_w are the convective heat transfer coefficients of the hot side and the cold side, respectively, δ is thickness of heat transfer, λ is thermal conductivity, and ΔT_{lm} is the log mean temperature difference.

The Reynolds number is calculated by:

$$Re = \frac{\rho w D_h}{\mu} = \frac{2m}{\mu(W_c + D_c)} \quad (9)$$

The pressure drop due to friction is determined by

$$\Delta p = 2 f \rho w^2 \frac{L}{D_h} = 2 f Re \frac{L}{D_h^2} w \mu \quad (10)$$

where $D_h = \frac{4A_c}{P}$ is the hydraulic diameter, w is velocity

in the z -direction, μ is dynamic viscosity, ρ is density, A_c

is cross-sectional area, P is wetted perimeter, L is channel length, and f is Fanning friction factor.

The performance index, ξ , is determined by

$$\xi = \frac{Q_w}{\Delta p} = \frac{m_w c_w (T_{w,o} - T_{w,i})}{\Delta p} \quad (11)$$

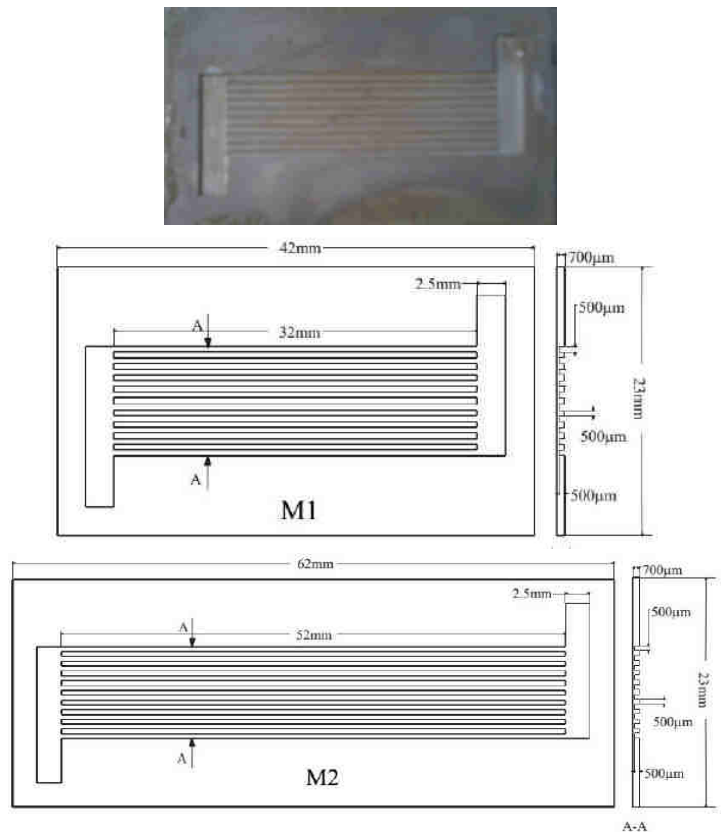


Fig. 1: Dimensions of models



Fig. 2: A photo of model M2

Two microchannel condensers were designed and tested in this study. Figure 1 shows the dimensions of the test sections. The material for the condensers is Aluminum, used as a substrate with thermal conductivity of 237 W/(mK), density of 2,700 kg/m³, and specific heat at constant pressure of 904 J/(kg K). Basically, the two models (M1 and M2) have the same dimensions; however, the channel length of M1 is 32 mm while M2 is 52 mm. Geometric parameters of microchannel condensers are listed in Table 1.

Table 1: Dimensions of models

No.	Dimensions of the substrate (mm)			Dimensions of the microchannel (μm)		
	L	W	T	L_c	W_c	D_c
M1	42	23	0.7	32,000	500	500
M2	62	23	0.7	52,000	500	500

For each microchannel condenser, the top side for the vapor has 10 microchannels and the bottom side for the cooling water also has 10 microchannels. All channels are connected with a manifold for each inlet or outlet of vapor and cooling water, respectively. The manifolds have a rectangular shape with the width of 2.5 mm and the depth of 500 μm . Figure 2 shows a photo of the microchannel condenser M2. These test sections were manufactured by precision micromachining. Each inlet or outlet of the condensers has cross-sectional area of 9 mm^2 . The four sides of the condenser were thermally insulated by the glass wool with a thickness of 5 mm. To seal the microchannels, two layers of PMMA are bonded on the top and bottom sides of the substrate, as indicated in Fig. 2. The physical properties of the PMMA (polymethyl methacrylate) and the glass wool are listed in Table 2. Accuracies and ranges of testing apparatus are listed in Table 3.

Material	Density kg/m^3	Thermal conductivity W/(mK)
PMMA	1420	0.19
Glass wool	154	0.051

Experimental setup

The test loop for the models is shown in Fig. 3. While experimenting, pressure was kept stably; buffer tank (9) and adjust valve (8) were installed after outlet steam of mini boiler (2). The vapor produced in the mini boiler passes through the microchannel condensers, where it transfers heat and condenses by the cooling water. To keep constant water level in boiler, the inlet water flow rate also held suitably with boiler capacity and adjusted by the mini pump (3). With the cooling water side, the mass flow rate of water was controlled by the pump (5). Experimental data for the microchannel condensers were obtained under the constant room temperature of 32 $^{\circ}\text{C}$. Each inlet or outlet of the heat exchanger has a set of two thermocouples to record temperature values, and there are seven thermocouples in total, as shown in Fig. 3. At each side, a differential pressure transducer was used to measure the pressure drop. All signals were recorded by a MX100 acquisition unit. To assess the accuracy of measurements presented in this work, the uncertainty values for measured parameters are listed in Table 3. Sensor positions are also indicated in Table 4.

Table 2: Physical properties of the PMMA and the glass wool

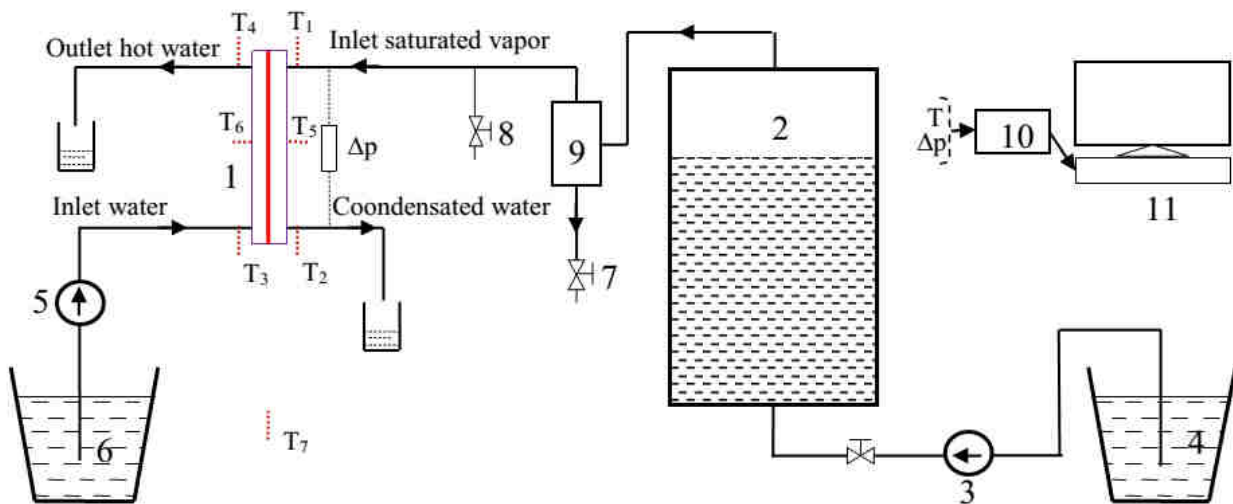


Fig. 3: Schematic of the test loop for the models

- 1. Microchannel condenser; 2. Electric mini Boiler; 3. Mini pump; 4. Water tank; 5. Cooling water pump; 6. Tank;
- 7. Condensing water valve; 8. Adjusting valve; 9. Buffer tank; 10. MX100 acquisition unit; 11. Computer.

Table 3: Uncertainty data for measured parameters

Parameter	Uncertainty
Temperature	± 0.1 $^{\circ}\text{C}$

Pressure	± 0.04 % FS
Mass flow rate	± 0.0015 g
Channel height	± 7 μm

Channel width	$\pm 10 \mu\text{m}$
Channel length	$\pm 70 \mu\text{m}$

Equipments used for the experiments are listed as follows:

1. Thermocouples, T-type
2. Pump, VSP-1200, made by Tokyo Rikakikai
3. Differential pressure transducer, Model PMP4110, made by Duck
4. Micro electronic balance, Model TE-214S, made by Sartorius.

Table 4: Sensor positions

Sensors	Positions	Measurement
Thermocouples: T - type	T ₁	Inlet vapor temperature
	T ₂	Condensing water temperature
	T ₃	Inlet cooling water temperature
	T ₄	Outlet cooling water temperature
	T ₅	PMMA surface temperature - vapor side
	T ₆	PMMA surface temperature - water side
	T ₇	Ambient temperature
Pressure different transducer	Δp	Pressure drop

III. RESULTS AND DISCUSSION

In this study, two microchannel condensers with difference in substrate length and channel length were evaluated. Experimental data for the microchannel condensers were obtained under the constant room temperature of 32 °C. The cooling water side was kept constantly at 31 °C. This study discussed on vapor side.

Figure 4 shows locations where appear condensation in microchannels for model M2. It is demonstrated that vapor condensation profiles in microchannels were depended on pressure drop; however, the pressure drop was depended on inlet steam flow rate. When pressure drop is low, oscillation of condensation profile is large (as shown in Figs. 4a – 4c), distance of beginning condensation point of the last channel to the manifold is slightly bigger than distance of beginning condensation point of the first channel to the manifold; however, when

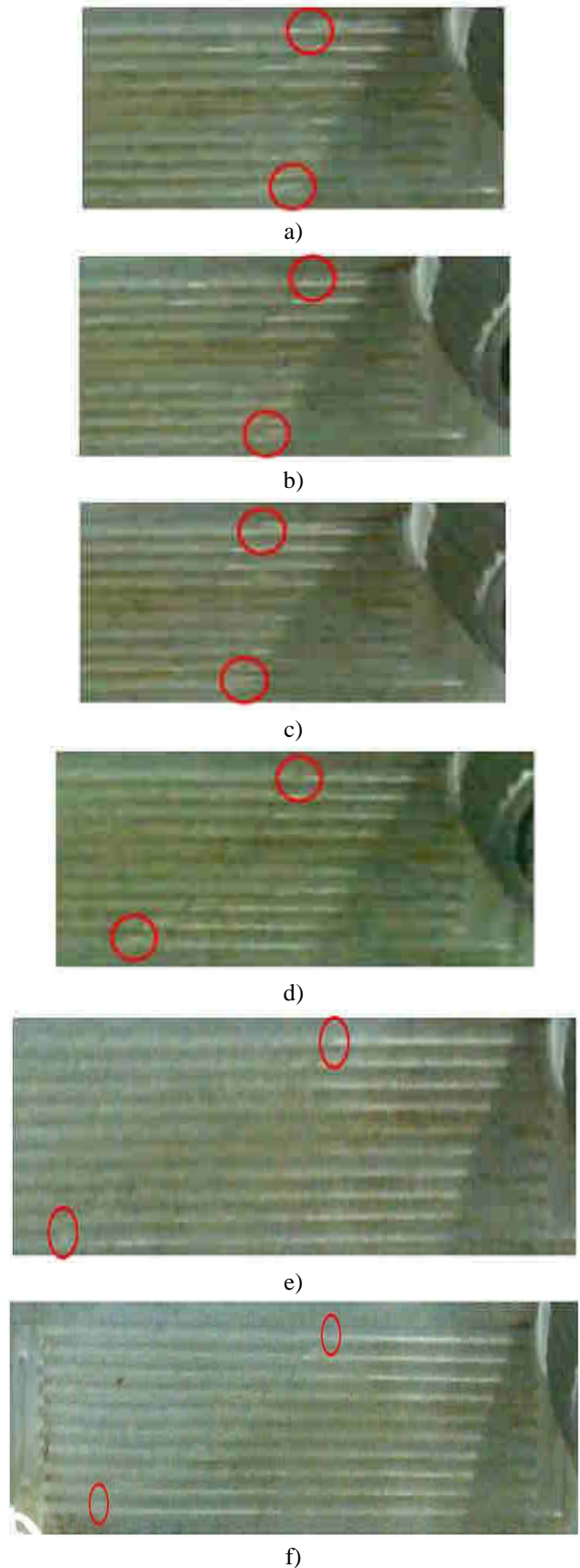


Fig. 4: Condensation profiles for the model M2 pressure drop increases, the oscillation decreases. When pressure drop strongly increases, distance of beginning

condensation point of the last channel to the manifold is more bigger than distance of beginning condensation point of the first channel to the manifold (as shown in Figs. 4d – 4f).

Figure 5 shows condensation profiles with four pressure drop values on vapor side of model M2. With pressure drop Δp_1 , condensation location of microchannel from No. 1 to 10 strongly oscillates in range 5 to 10 mm calculating from the left manifold. However, distance of condensation location of channel no. 1 to channel no. 10 strongly increases at 9.5 mm for Δp_1 , and 19.5 mm for Δp_4 , respectively.

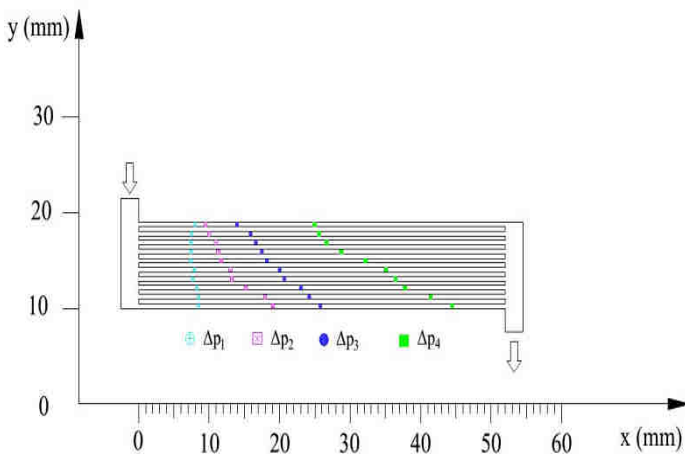


Fig. 5: Condensation positions versus pressure drop for the model M2
 ($\Delta p_1=6,105\text{Pa}$; $\Delta p_2=15,564\text{Pa}$; $\Delta p_3=30,599\text{Pa}$;
 $\Delta p_4=45,216\text{Pa}$)

Relationships between pressure drop and mass flow rate of steam of two microchannel condensers are shown in Fig. 6. It is observed that the pressure drop increases as the mass flow rate of steam increases. With the condenser M1, as mass flow rate of steam is increasing from 0.0264 g/s to 0.0721 g/s, the pressure drop increases from 1,257 Pa to 11,181 Pa, respectively. While, pressure drop of the condenser M2 strongly increases than of the condenser M1; with the condenser M2, as mass flow rate of steam is increasing from 0.0264 g/s to 0.0572 g/s, the pressure drop increases from 6,105 Pa to 45,216 Pa, respectively. The results from the Fig. 6 indicated that the pressure drop obtained from the microchannel condenser M1 is lower than that obtained from the microchannel condenser M2: at mass flow rate of 0.0264 g/s, the pressure drop of M1 is 1,257 Pa while the pressure drop of M2 is 6,105 Pa. The results demonstrated that pressure drop strongly depends on channel length of these microchannel condensers. In this study, the pressure drop of 45,216 Pa was achieved for the model M2, it is five times to compare with the model M1 as the same flow rate. The

results indicated that liquid viscosity is bigger than vapor viscosity, leading to pressure drop of model M2 is larger.

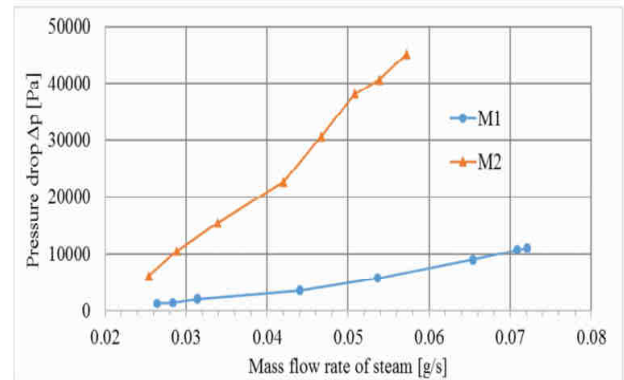


Fig. 6: Pressure drop versus mass flow rate of steam

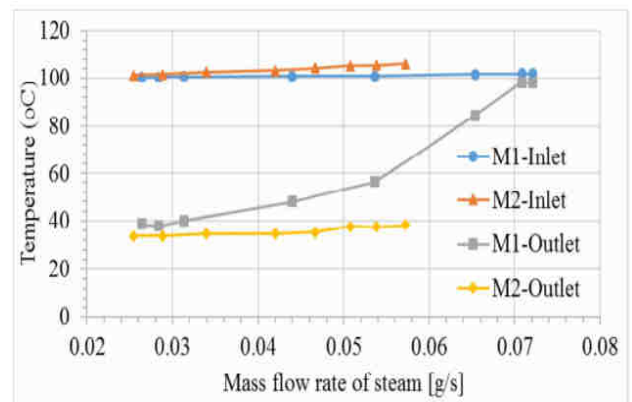


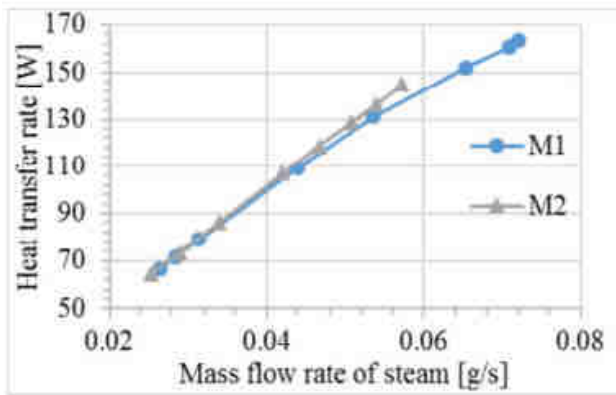
Fig. 7: Temperature versus mass flow rate of steam

Figure 7 shows a relationship between inlet/outlet vapor temperature and mass flow rate of steam of two microchannel condensers. With the model M1, when the mass flow rate of steam increases, the condensed water temperature strongly increases while the inlet vapor temperature constantly kept around 100.3 °C to 101.9 °C. With the model M2, the condensed water temperature slightly changes from 33.6 °C to 38.3 °C. The results demonstrated that microchannel length strongly effects to condensed water temperature.

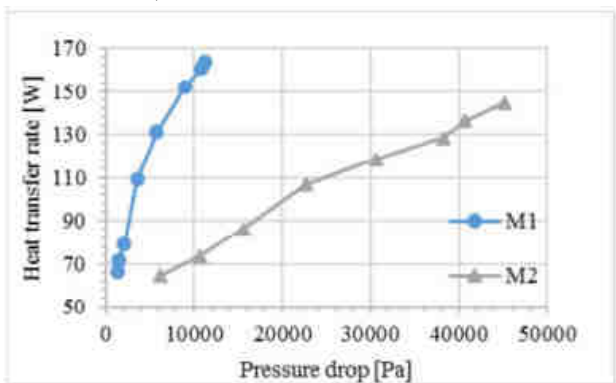
From Fig. 8, it is observed that heat transfer rate of model M1 is higher than that of model M2 at the same flow rate or pressure drop of steam. The heat transfer rate of 164 W was achieved for the model M1; 145 W, the model M2. The results obtained at inlet vapor temperature of 101.9 °C. The heat transfer rate of M1 is the highest in these experimental conditions.

The performance index of the condensers is shown in Fig. 9. The figure shown that the performance index obtained from the model M1 is higher than that obtained from the model M2. It means that the more channel length, the less performance. The performance decreases as rising mass flow rate of steam. With the microchannel condenser M1,

the performance index is decreasing from 0.053 to 0.038 as varying mass flow rate of steam from 0.0264 g/s to 0.0314 g/s. The performance indexes linearly decrease for both condensers.



a) With mass flow rate of steam



b) With pressure drop

Fig. 8: Heat transfer rate

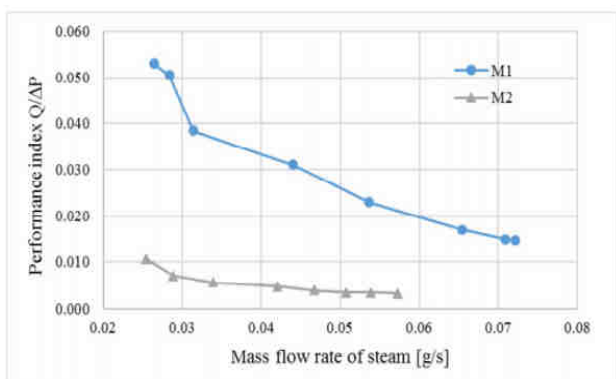


Fig. 9: Performance index versus mass flow rate of steam

IV. CONCLUSION

An experimental study on condensation in horizontal microchannels was done. In this study, two microchannel condensers have the same dimensions; however, they have different substrate and channel lengths.

When pressure drop is low, oscillation of condensation profile is large, distance of beginning condensation point

of the last channel to manifold is slightly larger than distance of beginning condensation point of the first channel to manifold; however, when pressure drop increases, the oscillation decreases, distance of beginning condensation point of the last channel to manifold is more larger than distance of beginning condensation point of the first channel to manifold.

Besides, the pressure drop obtained from the microchannel condenser M1 is lower than that obtained from the microchannel condenser M2: at mass flow rate of 0.0264 g/s, the pressure drop of M1 is 1,257 Pa while the pressure drop of M2 is 6,105 Pa.

In addition, the performance index decreases as rising mass flow rate of steam. With the microchannel condenser M1, the performance index is decreasing from 0.053 to 0.038 as varying mass flow rate of steam from 0.0264 g/s to 0.0314 g/s. The performance indexes decrease linearly for both condensers.

ACKNOWLEDGEMENTS

The supports of this work by the project No. T2015-50TD/KHCN-GV (sponsored by the specific research fields at Hochiminh City University of Technology and Education, Vietnam) is deeply appreciated.

REFERENCES

- [1] Aritra Sur, Dong Liu. Adiabatic air-water two-phase flow in circular microchannels. International Journal of Thermal Sciences 53 (2012) 18-34.
- [2] C.W. Choi, D.I. Yu, M.H. Kim. Adiabatic two-phase flow in rectangular microchannels with different aspect ratios: Part I – Flow pattern, pressure drop and void fraction. International Journal of Heat and Mass Transfer 54 (2011) 616–624.
- [3] C.W. Choi, D.I. Yu, M.H. Kim. Adiabatic two-phase flow in rectangular microchannels with different aspect ratios: Part II – bubble behaviors and pressure drop in single bubble. International Journal of Heat and Mass Transfer 53 (2010) 5242–5249.
- [4] Jaehyeok Heo, Hanvit Park, Rin Yun. Comparison of condensation heat transfer and pressure drop of CO₂ in rectangular microchannels. International Journal of Heat and Mass Transfer 65 (2013) 719–726.
- [5] Hicham El Mghari, Mohamed Asbik, Hasna Louahlia-Gualous. Condensation Heat Transfer in Horizontal Non-Circular Microchannels. Energy and Power Engineering, 2013, 5, 577-586.
- [6] Hicham El Mghari, Mohamed Asbik, Hasna Louahlia-Gualous, Ionut Voicu. Condensation heat transfer enhancement in a horizontal non-circular microchannel. Applied Thermal Engineering 64 (2014) 358-370

- [7] X.J. Quan, P. Cheng, H.Y. Wu. An experimental investigation on pressure drop of steam condensing in silicon microchannels. *Int. J. Heat Mass Transfer* 51 (2008) 5454–5458
- [8] Xiaojun Quan, Lining Dong, Ping Cheng. Determination of annular condensation heat transfer coefficient of steam in microchannels with trapezoidal cross sections. *International Journal of Heat and Mass Transfer* 53 (2010) 3670–3676.
- [9] Thanhtrung Dang and Minhhung Doan, An Experimental Investigation on Condensation Heat Transfer of Microchannel Heat Exchangers, *International Journal of Computational Engineering Research*, Vol 03, Issue 12, 2013, pp25-31.